LC-Note-DET-2001-014
January 15th, 2001

Pad readout geometries for a TPC with GEM readout for the TESLA linear collider.

Markus Schumacher, DESY

Abstract

A Time Projection Chamber (TPC) with Gas Electron Multiplier (GEM) readout is proposed to serve as the central tracking device for the detector at TESLA. In order to achieve the desired point resolution different pad geometries allowing improved charge sharing have been studied.

1 Introduction

In a conventional TPC [1] readout using wires stretched above readout pads, the wires act both to collect and amplify the charge from the primary ionisation drifting in the TPC volume, and to induce charge on the readout pads. The induction mechanism results in charges on several readout pads close to the wire, giving a position resolution much better than $\Delta\phi/\sqrt{12}$, where $\Delta\phi$ is the pad pitch in the azimuthal direction. The width of the signal spreading over several pads is dominated by the geometry of the readout chamber.

If the wire readout is replaced by a cascade of GEMs [2], again above a plane of readout pads, the induction mechanism no longer operates. The electron are collected directly by the readout pads. The width of the electron cloud is given by the transverse diffusion in the gas volume and therefore depends on the drift length of the primary electrons. For short drift length all electrons will be collected on one rectangular shaped pad and no centre-of-gravity algorithm can be applied from the collected electron signal. Another idea is investigated by a group in Carleton using the induction signal on neighbouring pads created for a very short time during the amplication process [3].

The object of the present study is to evaluate alternative readout pad designs which will maximize charge sharing even for small drift distances and will reveal a modest dependence of the point resolution on the drift distance.

2 Pad Geometries

Three different shapes of pads have been investigated.

1. Rectangular Strips with $\Delta\phi = 1$ (2) mm and $\Delta r = 6$ mm.

2. Chevron shaped pads with $\Delta\phi = 1$ (2) mm and $\Delta r = 6$ mm.

3. Diamond shaped pads with $\Delta\phi = 1$ (2) mm and $\Delta r = 6$ mm.

The different pad geometries are shown in figure 1. The chevrons and diamonds shown have 2 'zigzags'. In addition 8 and 32 'zigzags' have also been studied. The area of a single pad corresponds to 6 (12) mm^2. This determines the number of readout channels to $2\times$ 1.26 (0.64) $\times 10^6$ assuming the TPC to extend from 40 cm to 160 cm radially and from -250 to 250 cm along the z-direction.

3 Simulation method

The simulations used a simple standalone program [4], calculating the response of a single row of pads on the TPC endplate to a track passing through the drift volume. The simulation proceeds through the stages described below. The

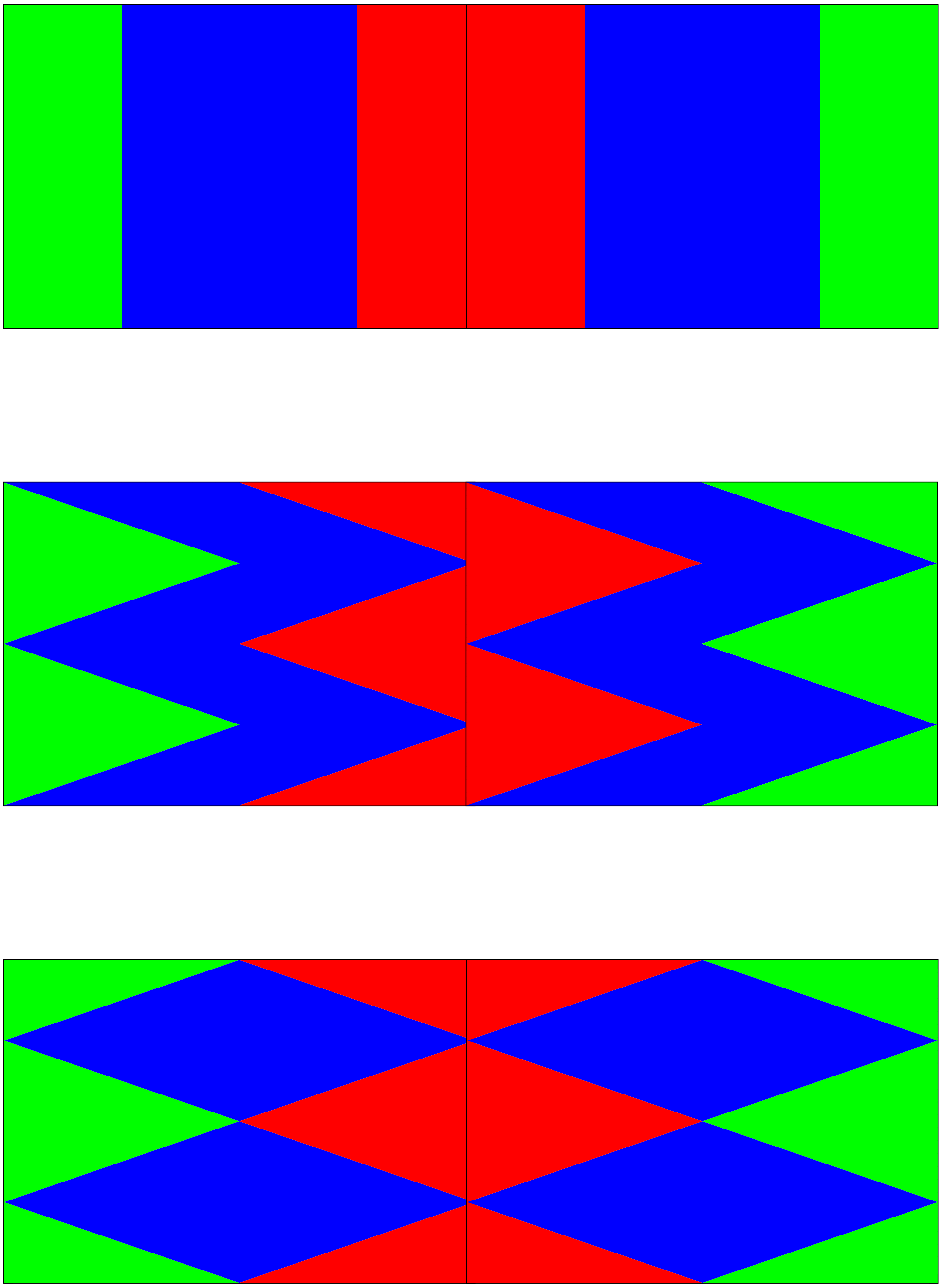

Figure 1: *Different pad geometries (extract from one pad row in ϕ direction, not to scale): top: rectangular strips, middle: chevron shaped pads, bottom: diamond shaped pads.*

evaluation was done for two gas choices (a) 90 % Ar, 10,% CH_4 (similar to the ALEPH gas composition) and (b) 93 % Ar, 5 % CH_4, 2 % $C0_2$ currently used in the DESY TCP setup and recommended by the gas studies [5] and a magnetic field of 4 Tesla. The transverse diffusion coefficients for the two gas mixtures are (a) $D_t(4T) = 40\ \mu$m and (b) $D_t(4T) = 70\ \mu$m [6]. These values are valid for the field strength which maximises the drift velocity in the particular gas mixture. The length of one half of the TPC is 250 cm and the readout is performed by a cascade of two GEMs with hole pitch of 140 μm. The two GEMs and the pad plane are each separated by a gap of 1 mm. The simulation proceeds in the following steps:

1. **Drift volume**
   A position for the track across the pad row x is chosen at random, and the trajectory calculated. For most runs the tracks were produced at normal incidence. Primary ionisation clusters are then produced along the length of the track above the pad row. The clusters are produced randomly, with an average multiplicity of $N_{\rm clus} = 33$ clusters/cm, and an average of $N_{e^-/clus} =$ 3 electrons per cluster distributed according to Poissonian statistics. Each electron has its position smeared by a Gaussian distribution with width of $\sigma = D_t \times l_{drift}$, simulating transverse diffusion in the drift volume between the track and the TPC endplate.

2. **GEM 1**
   The drifted electrons are moved to the centre of the 'nearest' hole in the first GEM foil. Thus the information on whether the electron was close to the centre of a hole or between holes is lost, simulating the 'focusing' of all drift electrons into the GEM holes. Amplification in the GEM is simulated with an average gain of 70 where the fluctuations of gain follow an exponential law. The secondary electrons produced at the centre of each hole are smeared by another Gaussian distribution with rms = 100 μm, to simulate diffusion in the transfer gap. The rms corresponds to the transverse diffusion for a gap of 1 mm in a magnetic field of 4 Tesla and electric field in the range of 1 to 4 kV/cm.

3. **GEM 2**
   The three steps as for GEM1 are repeated: forcing the charge to centre of the closest hole, amplification in the centre of the hole, applying smearing due to the diffusion in the induction gap

4. **Pad plane**
   The position of each secondary electron on the readout pad structure is calculated, and if it hits a readout pad, the charge is accumulated. Readout pads with charge above zero are then used to calculate the reconstructed x position, by a simple charge centre of gravity method. No cluster finding algorithm was applied, since only single tracks were simulated.

4 Results

The different pad geometries are compared with respect to their point resolution. For each track the residual between true ϕ-coordinate and reconstructed ϕ-coordinate are determined. The point resolution is defined as the width of the Gaussian fitted to the distribution of these residuals.

4.1 Point resolution dependence on drift length

The dependence of the point resolution on the drift length for various combinations of pad shapes, pad size and gas mixtures are shown in figures 2,3,4 and 5. The results are obtained for tracks at normal incidence.

Figure 2 compares the three pad designs for the two gas choices. Chevron and diamond shaped pads improve the pad resolution significantly for short drift distances. These two pad designs perform similarly well. For larger drift distances all pad structures perform equally well for the 1×6 mm^2 pad size. For the 2×6 mm^2 pad size chevrons and diamond shaped pads are doing better by about 20 μm for large drift distances.

A large difference in the achieved point resolution is observed between the two gas mixtures. For Ar:CH_4=(90:10)% the point resolution increases to 120 μm for full drift distance, for Ar:CH_4:CO_2=(93:5:2)% up to 215 μm.

The two different pad sizes are compared directly in figure 3. In the case of chevron and diamond shaped pads the point resolution for drift length larger than 50 cm depends only weakly on the pad width in azimuthal direction. The difference is smaller than 15 μm.

Figures 4 and 5 show the achieved point resolutions depending on the number of zigzags for chevron and diamond pad design, respectively. The performance improves significantly with the number of zigzags. The improvement is larger for broader pads and gas mixtures with smaller diffusion coefficients.

4.2 Point resolution dependence on pad crossing angle

The dependence of the point resolution on the pad crossing angle are shown in 6 for a drift length of 40 cm and in figure 7 for a drift length of 250 cm. Diamond shaped pads show the same behaviour as chevron shaped and are therefore omitted from the figures. For the choices of gas mixtures and pad geometry which give satisfying results for normal incidence the resolution worsens with the size of the track pad angle. No sigificant preference for the gas choice and pad geometries can be deduced from the simulation results.

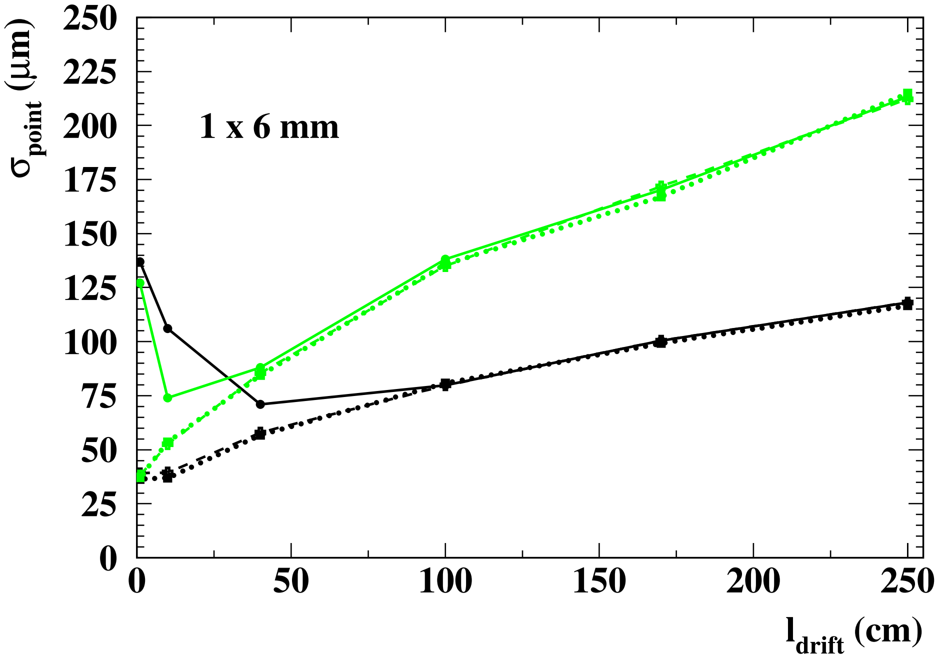

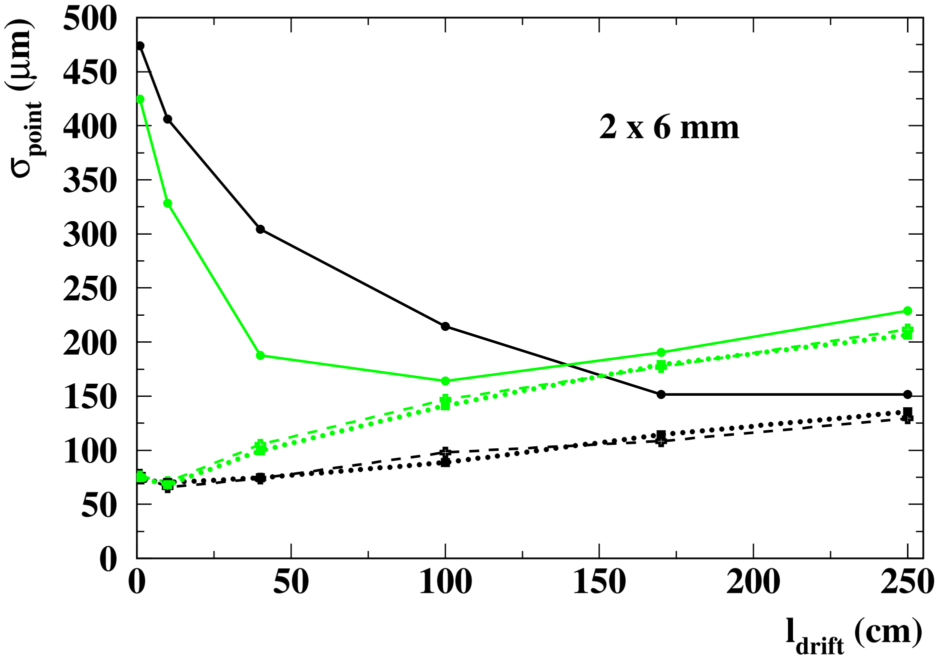

Figure 2: *Point resolution dependence on drift length: pad size 1×6 mm^2 top, 2×6 mm^2 bottom. Solid curve strips, dashed chevrons (8 zigzags), dotted diamond (8 zigzags). Dark curves for Ar:CH_4 = (90:10)%, light curves for Ar:CH_4:CO_2 = (93:5:2)%*

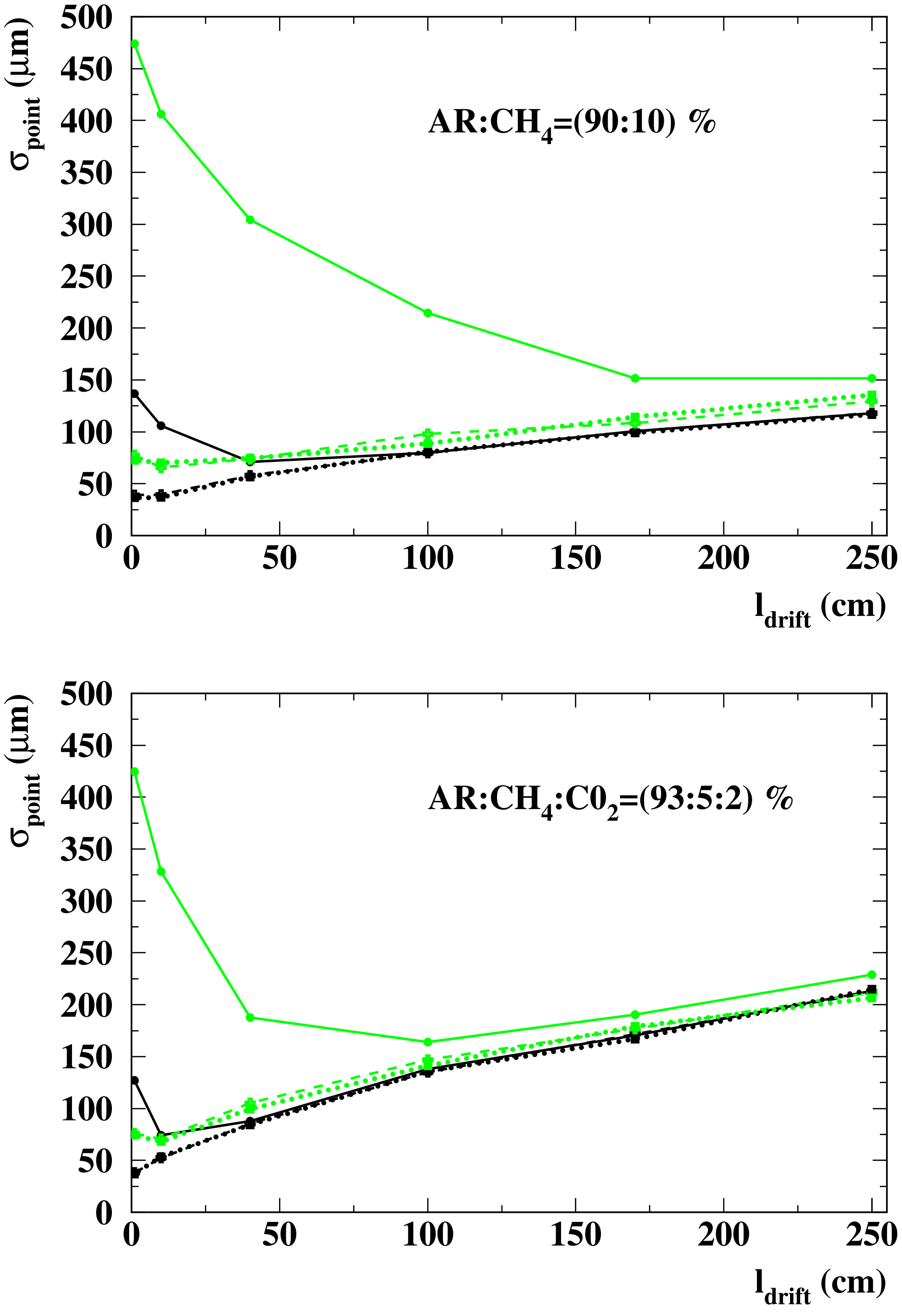

Figure 3: *Point resolution dependence on drift length: Ar:CH_4 = (90:10)% top, Ar:CH_4:CO_2 = (93:5:2)% bottom. Solid curve strips, dashed chevrons (8 zigzags), dotted diamond (8 zigzags). Dark curves for pad size 1×6 mm^2, light curves for 2×6 mm^2*

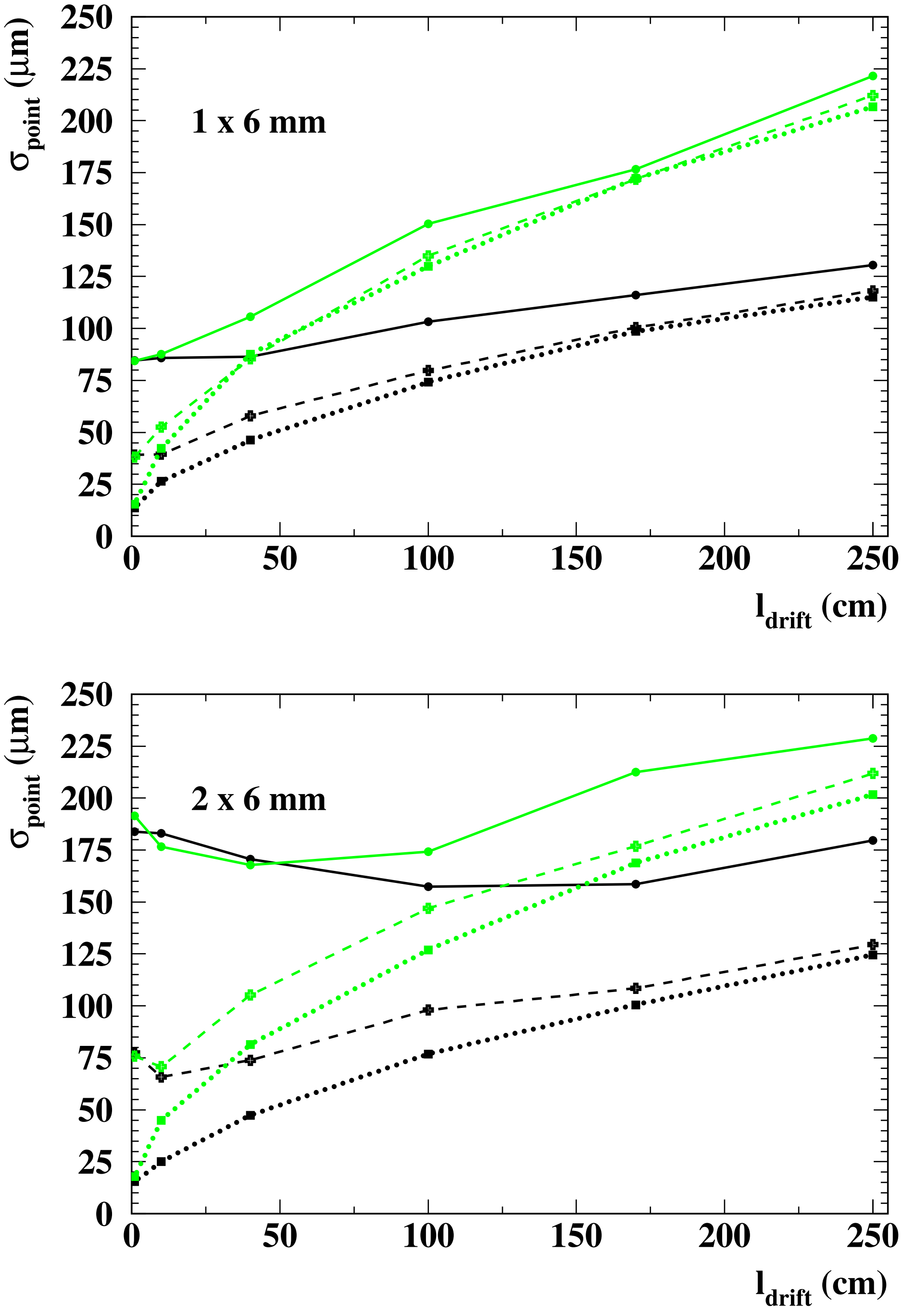

Figure 4: *Point resolution dependence on drift length for chevron pads with different number of zigzags: pad size 1×6 mm^2 top, 2×6 mm^2 bottom. Solid curve 2 zigzags, dashed 8 zigzags, dotted 32 zigzags. Dark curves for Ar:CH_4 = (90:10)%, light curves for Ar:CH_4:CO_2 = (93:5:2)%*

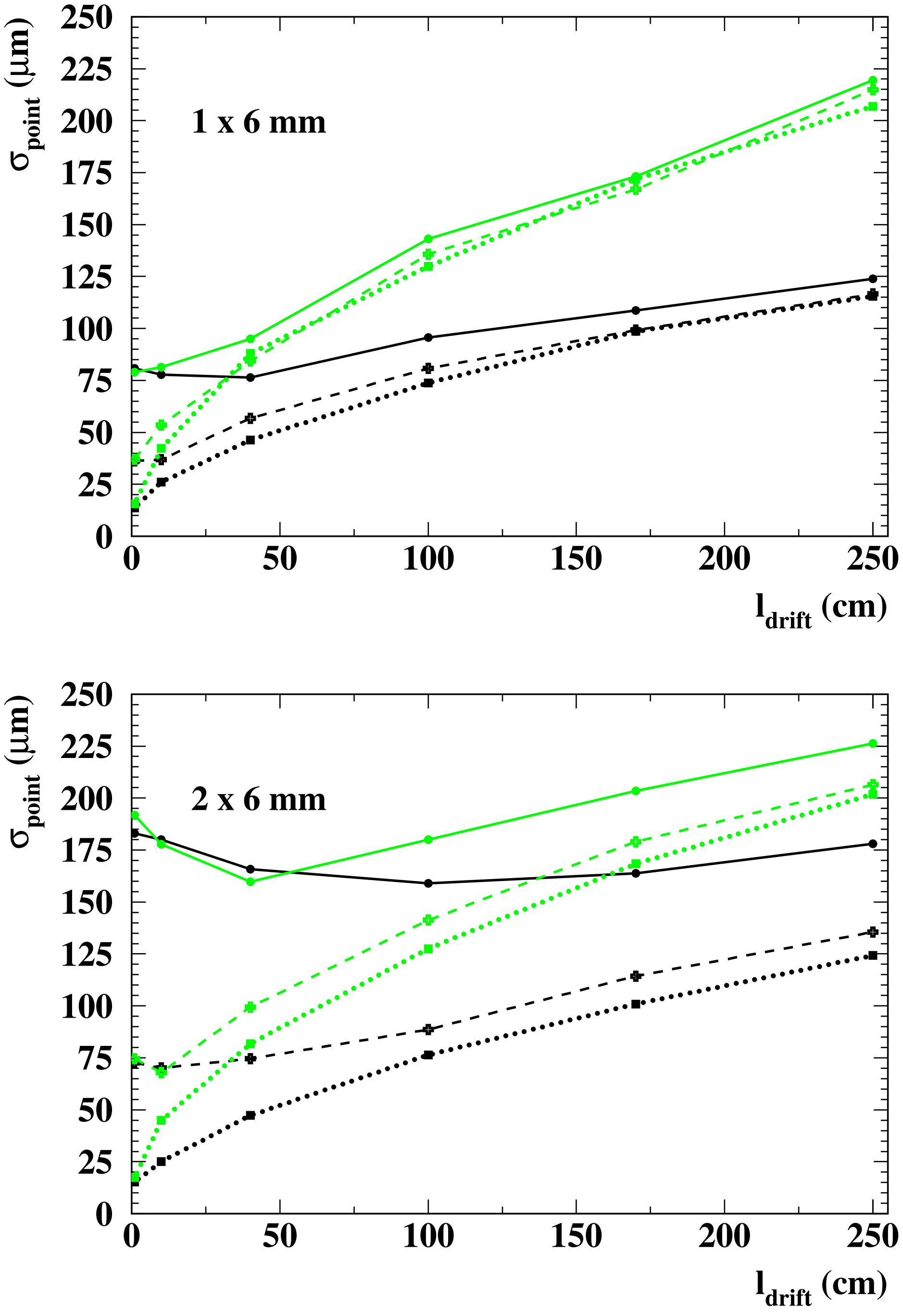

Figure 5: *Point resolution dependence on drift length for diamond pads with different number of zigzags: pad size 1×6 mm^2 top, 2×6 mm^2 bottom. Solid curve 2 zigzags, dashed 8 zigzags, dotted 32 zigzags. Dark curves for Ar:CH_4 = (90:10)%, light curves for Ar:CH_4:CO_2 = (93:5:2)%*

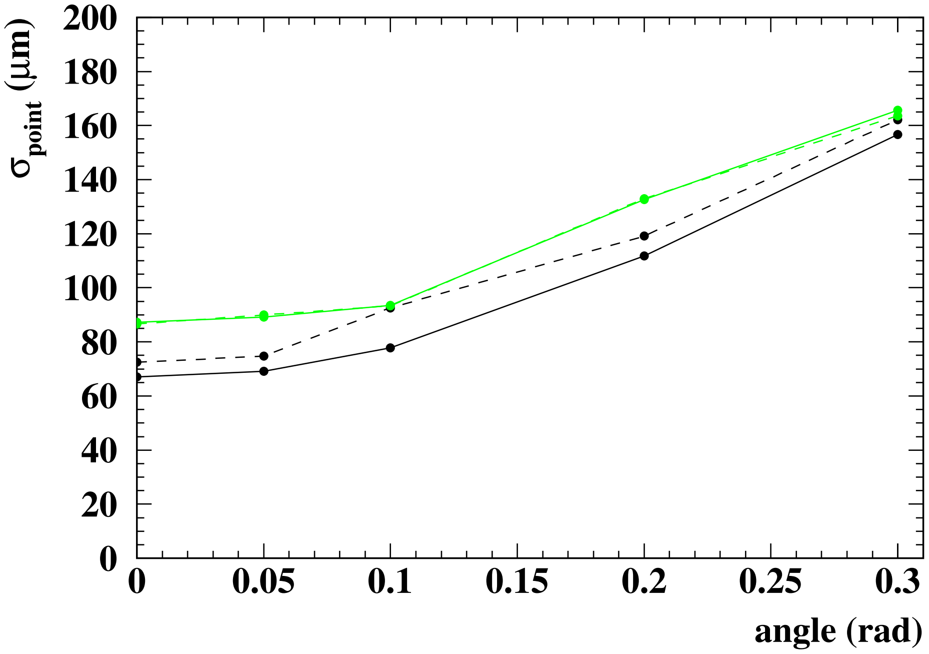

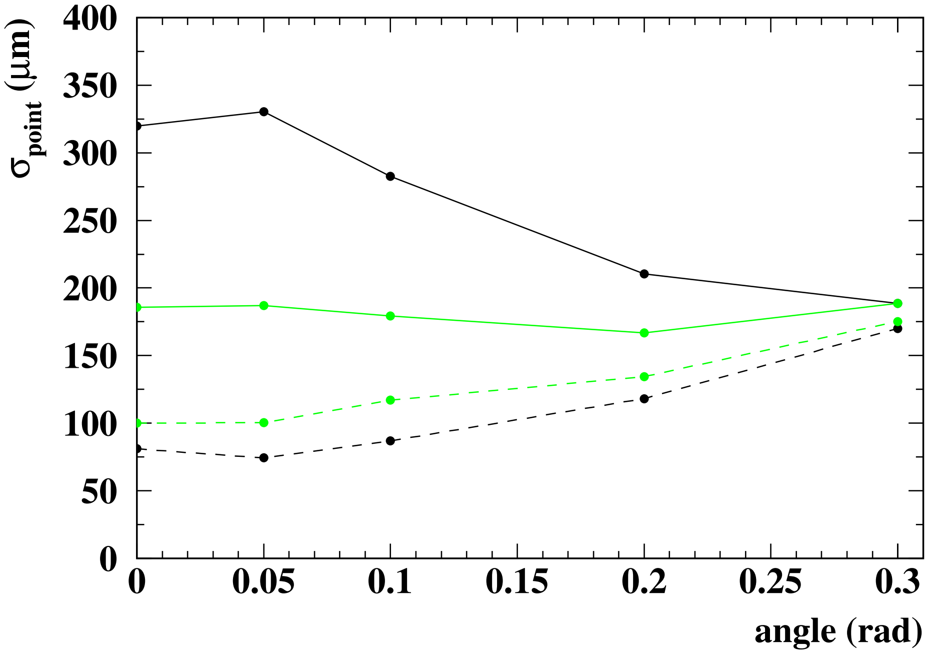

Figure 6: *Point resolution dependence on crossing angle for drift length of 40 cm: pad size* 1×6 *mm*^{2} *top,* 2×6 *mm*^{2} *bottom. Solid curve strips, dashed chevrons (8 zigzags). Dark curves for* $Ar{:}CH_4 = (90{:}10)\%$*, light curves for* $Ar{:}CH_4{:}CO_2 = (93{:}5{:}2)\%$

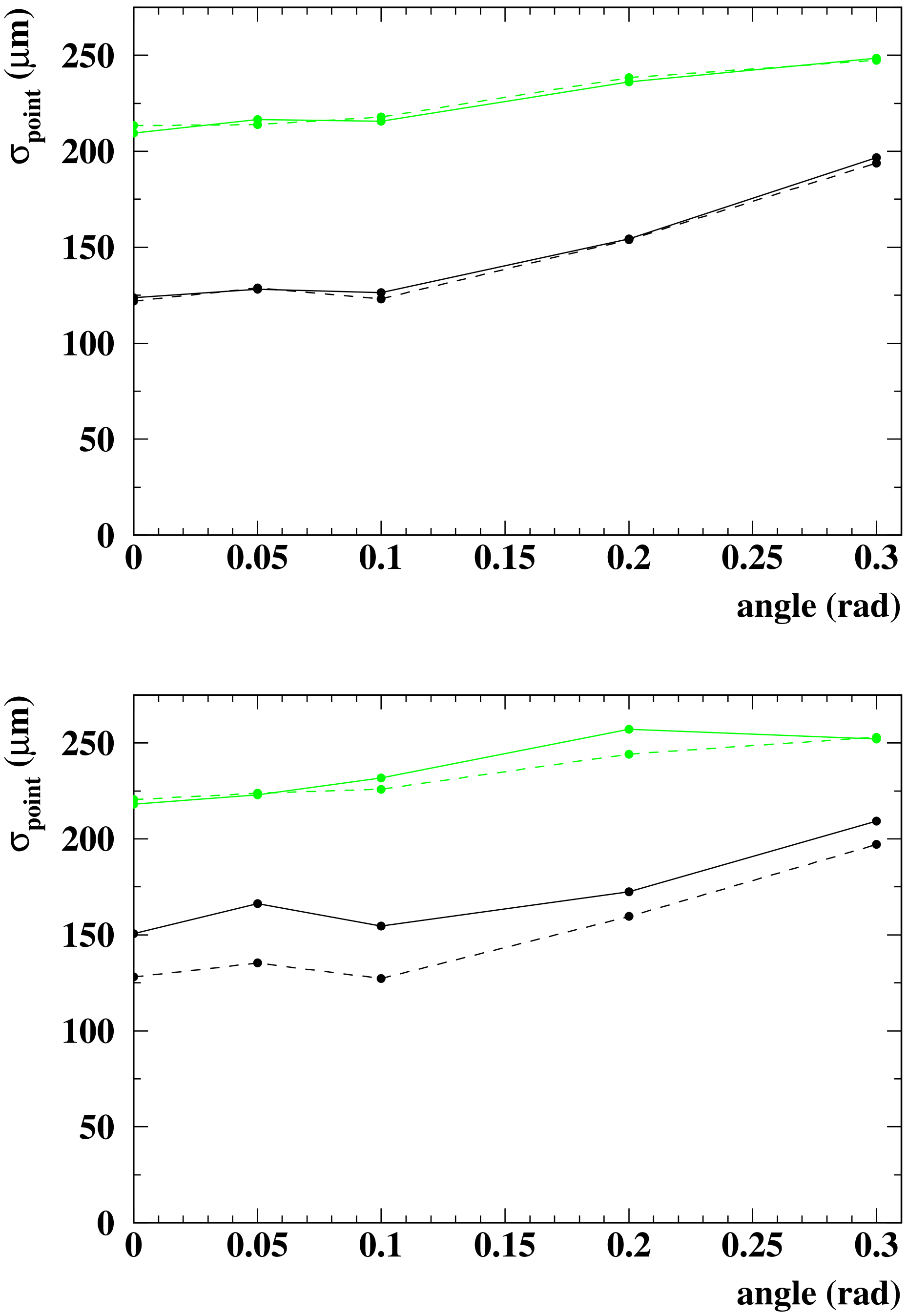

Figure 7: *Point resolution dependence on crossing angle for drift length of 250 cm: pad size 1×6 mm^2 top, 2×6 mm^2 bottom. Solid curve strips, dashed chevrons (8 zigzags). Dark curves for Ar:CH_4 = (90:10)%, light curves for Ar:CH_4:CO_2 = (93:5:2)%*

5 Conclusion

The influence of different pad design options on the point resolution for the proposed TPC with GEM read out at TESLA has been studied.

It has been found that more sophisticated pad structures like chevron or diamond shaped pads improves the charge sharing capabilities and therefore the point resolution for small drift distances. The dependence on the drift length can be flattened compared to the behaviour of simple rectangular strips. The results for chevron and diamond shaped pads depend only weakly on the azimuthal pad size. The choice of 2×6 mm pads seems fine from the performance point of view and preferable with respect to packing density of the electronics and number of readout channels. A large dependence on the gas mixtures is observed. The composition Ar:CH_4:CO_2 = (93:5:2)% gives point resolutions up to 215 μm, whereas Ar:CH_4 = (93:10)% stays below 120 μm. It may be worth to reconsider the questions of gas choice taking into account this result together with the properties concerning background especially neutron crosssection.

However, both gas mixtures for both pad sizes and chevron and diamond shaped pads meet the performance goal [7] of a momentum resolution $\sigma(1/p_t) = 6\times10^{-6}$ (1/GeV) for the whole TESLA tracking system. This has been verified by using the point resolution results from this study as input for the simulation of TPC in the BRAHMS package [8].

6 Acknowledgements

Richard Hawkings is greatfully acknowledged for the introduction into the topic, providing a first version of the simulation program and numerous helpful discussions.

References

[1] D. R. Nygren, *The Time Projection Chamber: A new 4 pi detector for charged particles.*, PEP-0144, Proceedings, Pep Summer Study, Berkeley 1975, page 58-78.

[2] F. Sauli, *GEM: A new concept for electron amplification in gas detectors*, Nucl. Instru. and Meth. **A386**, (1997), 531.

[3] M. Dixit, D. Karlen et al., *R&D in Carleton University*, LC-NOte to be written 2001; D. Karlen, *Studies of GEMs with hexagonal pads*, talk given at Linear Collider Workshop 2000 - LCWS 2000, Oct. 2000.

[4] R. Hawkings, first version of the simulation program, private communication.

[5] M. Gruwe, *Gas Studies for a TPC of a detector for the future linear collider TESLA*, LC-DET-1999-003.

[6] M. Gruwe, *private communication.*

[7] R. Brinkmann and G. Materlik and J. Rossbach and A. Wagner (ed.), *Conceptual Design of a 500 GeV e^+e^- Linear Collider with Integrated X-Ray Laser Facility*, DESY 1997-048, ECFA 1997-182.

[8] T. Behnke, G. Blair et al., *BRAHMS: A Monte Carlo for a Detector at a 500/800 GeV Linear Collider*, LC-TOOL-2001-005;
http://www.hep.ph.rhcbn/ac.uk/ blair/detsim/brahms.html.